Available online at www.sciencedirect.com
ScienceDirect
Catalysis Today 122 (2007) 78–90
CATALYSIS TODAY
www.elsevier.com/locate/cattod

Dimensionless analysis of slurry photocatalytic reactors using two-flux and six-flux radiation absorption–scattering models

Gianluca Li Puma [a,*], Alberto Brucato [b]

[a] Photocatalysis & Photoreaction Engineering, School of Chemical, Environmental and Mining Engineering (SChEME), The University of Nottingham, University Park, Nottingham NG7 2RD, United Kingdom
[b] Dipartimento di Ingegneria Chimica dei Processi e dei Materiali (DICPM), Universita' degli Studi di Palermo, Viale delle Scienze, 90128 Palermo, Italy

Available online 31 January 2007

Abstract

This paper presents a dimensionless analysis of steady-state, continuous flow, photocatalytic reactors using ''two-flux'' (i.e., scattered photons are purely back scattered) and ''six-flux'' (i.e., scattered photons follow the route of the six directions of the Cartesian coordinates) radiation absorption–scattering models. The models retain the essential elements of a rigorous approach, whilst providing simple solutions. The effect of scattering albedo, ω and ''apparent'' optical thickness, τ_{app}, over reactant conversion in a flow-through photocatalytic reactor was analysed using the above models for three ideal flow conditions: (1) falling film laminar flow, (2) plug flow and (3) slit flow.

The model simulations show that the optimum value of τ_{app} that maximizes the conversion is a complex function of fluid flow and reaction kinetics and should be found in the range from 1.8 to 4.4. When comparing the models to experimental results for the photocatalytic oxidation of the herbicide ''isoproturon'' in a recirculation batch reactor, significant errors in predicting reactant conversion were found when neglecting the full effect of the radiation scattering phenomena. The experimental results were enclosed by the Beer–Lambert absorption model and the two-flux radiation model; however, the six-flux model provides the most accurate, yet simple, analysis of the radiation field in a photocatalytic reactor.

Keywords: Photocatalysis; Photocatalytic reactors; Radiation scattering; Thin film; Annular; Titanium dioxide

1. Introduction

Photocatalytic oxidation (PCO) is a highly effective process for the degradation and mineralization of a wide variety of priority pollutants in lightly contaminated water and wastewater [1–4]. The absorption of UV radiation by a semiconductor photocatalyst in the presence of adsorbed water and an electron acceptor yields highly reactive hydroxyl radicals. The hydroxyl radical is the second most powerful oxidant after fluorine and is believed to be the main species responsible for the oxidation of organic substrates is solution. The most commonly used photocatalyst is titanium dioxide (TiO_2), which is inexpensive, abundant, photostable and non-toxic.

Among the different types of scalable photocatalytic reactors proposed in the literature using suspended solid photocatalysts, falling film or double-skin annular/slab reactors are the most common [5–7]. These reactor types have been used in the majority of studies presented in the literature for either kinetics studies or for assessing the potential of using photocatalysis for environmental applications.

Reliable tools for the design and modeling of heterogeneous photoreactors are required in order to successfully bring photocatalytic processes to the stage where they can be adopted by industry. They are also required to determine accurate kinetic parameters from experimental laboratory reactors.

Modeling of photocatalytic reactors is a highly complex task which requires an intricate analysis of the radiation field in the photoreactor [8–10]. This analysis, linked to the modeling of the fluid-dynamics and the reaction kinetics, results in integro-differential equations which require demanding numerical computations. Simplified mathematical models that retain the essential elements of a rigorous model and that can be readily used for scale-up, design and optimization are therefore desirable.

This paper presents a dimensionless analysis of steady-state, continuous flow, photocatalytic reactors using suspended solid

* Corresponding author. Tel.: +44 115 951 4170; fax: +44 115 951 4115.
E-mail address: gianluca.li.puma@nottingham.ac.uk (G. Li Puma).

0920-5861/$ – see front matter
doi:10.1016/j.cattod.2007.01.027

Nomenclature

a	model parameter SFM
A	geometrical coefficient
b	model parameter SFM
c_{cat}	photocatalyst concentration (kg m^{-3})
C	substrate concentration (kg m^{-3})
H	length of the reactor (m)
I	radiation intensity (or radiative flux) (W m^{-2})
I_λ	radiation intensity divided by wavelength of radiation (W m^{-3} nm^{-1})
$I^{max}_{\xi=0}$	maximum value of radiation intensity at surface $\xi = 0$ (W m^{-2})
$I^*_{\xi^*,z^*}$	dimensionless radiation intensity or dimensionless LVRPA ($= I_{\xi,z}/I^{max}_{\xi=0}$)
k_T	kinetic constant (kg$^{(1-n)}$ s^{-1} W^{-m} m$^{(3m+3n-3)}$)
L	lamp length (m)
(LVRPA)	local volumetric rate of photon absorption (W m^{-3})
(LVRPA)*	dimensionless local volumetric rate of photon absorption ($=$ (LVRPA)/(LVRPA)$^{max}_{\xi^*=0}$)
m	order of the reaction with respect to the LVRPA
n	order of the reaction with respect to substrate concentration
N_{Da}	Damköhler number
N_{Re}	Reynolds number
p_b	probability of scattering in the backward direction
p_f	probability of scattering in the forward direction
p_s	probability of scattering in the side direction
r	radial coordinate (m)
r^*	dimensionless radial coordinate ($=r/R$)
r_l	lamp radius (m)
r_j	rate of the reaction with respect to substrate j (kg s^{-1} m^{-3})
R	external radius of annulus (m)
S	radiation emission of lamp per unit time per unit length (W m^{-1})
v	fluid velocity (m s^{-1})
V	reactor volume (m^3)
W	radiant power (W)
z	axial coordinate (m)
z^*	dimensionless axial coordinate ($=z/H$)

Greek letters

α	geometrical parameter ($=H/L$)
β	geometrical parameter ($=L/\eta R$)
δ	thickness of the annulus (m)
Φ	scattering phase function
γ	dimensionless parameter SFM
φ	scattering angle
η	ratio of internal radius to external radius of annulus
κ	specific mass absorption coefficient averaged over the spectrum of the incident radiation (m^2 kg^{-1})
λ	radiation wavelength (m)
ν	kinematic viscosity (m^2 s^{-1})
σ	specific mass scattering coefficient averaged over the spectrum of the incident radiation (m^2 kg^{-1})
τ	optical thickness
τ_{app}	apparent optical thickness
ω	scattering albedo ($=\sigma/(\sigma+\kappa)$)
ω_{corr}	corrected scattering albedo SFM
ξ	film thickness coordinate (m)
ξ^*	dimensionless film thickness coordinate ($=\xi/\delta$)
ψ	dimensionless parameter in the TFM
Ψ	radiation transmission factor

Subscripts

abs	absorbed
j	substrate
l, lamp	lamp
min	minimum
max	maximum
λ	wavelength
r, r*	direction along the radial coordinate
ηR	position at inner wall of annulus
w	lamp wall
z, z^*	direction along the axial coordinate
ξ, ξ^*	direction along the film transversal coordinate

Superscripts

*	dimensionless variable
H^*	reactor outlet position
in	position at inlet of the reactor
max	maximum value
out	position at outlet of the reactor

photocatalysts that still retains the essential elements of a rigorous modeling approach, whilst providing simple solutions. Three different levels of complexity for the models have been developed depending on whether radiation scattering is a relevant phenomena and whether the reactor is ''thin-film'' or ''geometrically thick'' type. To address these effects the radiation field in the photoreactor is modelled with either a ''two-flux'' absorption–scattering model [11–13], i.e., scattered photons are purely back scattered, or a ''six-flux'' absorption–scattering model [14,15], i.e., scattered photons follow the route of the six directions of the Cartesian coordinates. The models developed are applicable to either ''thin-film'' or ''geometrically thick'' slab and annular geometries, of (a) falling film design or (b) double-skin design, operating with three ideal flow conditions: (1) falling film laminar flow (FFLF), (2) plug flow (PF) and (3) slit flow (SF). The effect of the dimensionless parameters over reactor conversion is presented and discussed. The models were applied to the PCO of the herbicide ''isoproturon'' [3-(4-isopropylphenyl)-1,1-dimethylurea] in an experimental reactor and the uncertainty in predicting the experimental results is shown.

It is worth noting that photocatalysis may well be employed for treating gas streams in solid–gas reactors. In this case

photocatalyst particles are usually attached to solid walls, rather than being freely suspended in the fluid phase. This clearly requires different modelling tools than those adopted in the present paper, which is therefore mainly aimed at analysing the performance of solid–liquid (slurry) photoreactors.

2. Modeling of photocatalytic reactors

A schematic representation of the general methodology for the modeling of a photocatalytic reactor has been shown in the literature [16]. The development of a complete reactor model requires the inclusion of a number of sub-models. These are a radiation emission/incidence model, a radiation absorption–scattering model, a kinetic model and a fluid-dynamic model. The central aspect of the modeling procedure is however, the calculation of the local volumetric rate of photon absorption (LVRPA) at each point of the reaction space, which in the most complex case requires solving the radiative transfer equation (RTE) in the reaction space [9]. As a result of the complex nature of radiation scattering, this results in a set of integro-differential equations, which require elaborate numerical methods, especially in curvilinear co-ordinate systems.

Due to their absorbance spectra and/or their low concentration, the absorption of photons by the species in solution is often negligible in comparison with that of the photocatalyst. In such cases direct photolysis of the species can be neglected and it can be safely assumed that the photons with energy higher than the band-gap of the semiconductor are absorbed by the solid photocatalytic particles only.

This assumption removes the interdependence of the progress of the reaction and the attenuation of the radiation from the species in solution because the photocatalyst does not undergo changes in concentration. Consequently, the radiation field can be decoupled from the reactant concentration field and can therefore be computed in advance.

Once the LVRPA has been calculated, it is normally substituted into the kinetic equation, and the material balance for the substrate j in the reactor is solved with suitable initial conditions, to estimate the concentration of j at the reactor outlet.

Three approaches have been proposed in the literature for the calculation of the LVRPA: (1) the ''rigorous approach'' which involves the mathematical solution of the RTE, although its integro-differential nature makes this approach significantly complex [8–10]; (2) the ''numerical approach'' which involves the Monte Carlo simulation of the radiation field in the photoreactor, a simple but also a computationally demanding procedure [17]; and (3) strongly simplified radiation field models such as the Zero Reflectance Model (ZRM) [18] and the Two Flux Model (TFM) [11–13] that, although approximate, give an immediate grasp and physical understanding of the role played by the key parameters in the whole process. The former is based on the assumption of no photon scattering by the photocatalytic particles while the latter assumes that photon scattering can occur in the backward direction only. Recently a novel simplified ''Six-Flux Model'' (SFM) was also proposed [14,15], which has been shown to be able to match quite closely the exact solution of the RTE, while still retaining all the advantages of simplified models.

The two- and six-flux models yield a sensible representation of the LVRPA in the reaction space and allow a considerable simplification of the mathematical model, as a result, these will be used in the present models.

For the sake of brevity this paper will present models for the annular geometrical configuration only. The models, however, can be easily translated to the slab geometry with appropriate changes in variables and coordinates and taking into account that the photon flux does not decrease with the inverse of distance in the slab geometry.

3. Modeling of annular photocatalytic reactors using suspended solid photocatalyst

A complete dimensionless mathematical model, which is straightforward to apply to steady-state, continuous flow, annular photocatalytic reactors using suspended solid photocatalysts is presented in Table 1. This model distinguishes between thin-film (TFS) and ''geometrically thick'' photoreactors, and exhibits three levels of complexity depending on the scattering properties of the photocatalyst (i.e., the value of the scattering albedo), and on the geometrical configuration of the photoreactor. The essential assumptions and features of this model are given below.

3.1. Reactor geometry and film thickness

A schematic representation of the geometry of an annular photocatalytic reactor is shown in Fig. 1, which shows a cross section of the cylindrical lamp and of the annulus in which the photocatalyst is suspended. The cylindrical symmetry of the configuration allows a two-dimensional analysis along the (r, z) plane to be made. The annulus has the following dimensions: external radius R, internal radius ηR, length H. A cylindrical UV lamp of length L is located in the axial centre of the annulus and centred with respect to the length of the reactor.

The reactor geometry of an annular photoreactor is described by the following dimensionless design parameters:

$$\alpha = \frac{H}{L} \tag{1}$$

$$\beta = \frac{L}{\eta R} \tag{2}$$

The dimensionless axial and radial coordinates are:

$$z^* = \frac{z}{H} \tag{3}$$

$$r^* = \frac{r}{R} \tag{4}$$

The dimensionless film thickness coordinate is:

$$\xi^* = \frac{\xi}{\delta} \tag{5}$$

where δ is the thickness of the annulus and ξ the film thickness coordinate with origin at the inner wall of the annulus.

Table 1
Dimensionless mathematical model for steady-state, continuous flow, annular photocatalytic reactors

Dimensionless geometrical parameters	$\alpha = \frac{H}{L}$; $\beta = \frac{L}{\eta R}$		
Reynolds number	$N_{Re} = \frac{2R(1-\eta)v_z^{\text{average}}}{\nu} = \frac{2\delta v_z^{\text{average}}}{\nu}$		
Dimensionless variables	$\xi^* = \frac{\xi}{\delta}$; $r^* = \frac{r}{R}$; $z^* = \frac{z}{H}$; $v_z^* = \frac{v_z}{v_z^{\max}}$; $C_j^* = \frac{C_j}{C_j^{\text{in}}}$; $(\text{LVRPA})^* = \frac{(\text{LVRPA})}{(\text{LVRPA})_{\xi^*=0}^{\max}} = I_{\xi^*,z^*}^* = \frac{I_{\xi,z}}{I_{\xi=0}^{\max}}$		
Scattering albedo	$\omega = \frac{\sigma}{\sigma+\kappa}$		
Optical thickness	$\tau = (\sigma+\kappa)c_{\text{cat}}\delta = (\sigma+\kappa)c_{\text{cat}}R(1-\eta)$		
Maximum radiation intensity at surface ($\xi^* = 0$)	$I_{\xi^*=0}^{\max} = f(\omega,\tau)\frac{r_1}{\eta R}\arctan\left(\frac{\beta}{2}\right)\int_{\lambda_{\min}}^{\lambda_{\max}} I_{w,\lambda}\,\mathrm{d}\lambda$		
Maximum LVRPA at surface ($\xi^* = 0$)	$(\text{LVRPA})_{\xi^*=0}^{\max} = \kappa c_{\text{cat}} I_{\xi^*=0}^{\max} = (1-\omega)\frac{\tau}{\delta} I_{\xi^*=0}^{\max} = (1-\omega)\frac{\tau}{R(1-\eta)} I_{\xi^*=0}^{\max}$		
Dimensionless radiation intensity at inner wall ($\xi^* = 0$)	$I_{\xi^*=0,z^*}^* = \frac{\arctan[(\beta/2)(2\alpha z^*-\alpha+1)]-\arctan[(\beta/2)(2\alpha z^*-\alpha-1)]}{2\arctan(\beta/2)}$		
Steady-state ideal flow systems	Thin-film annular photoreactors ($\eta \approx 1$)—FFLF ($N_{Re} < 750$): $v_z^* = 1-\xi^{*2}$, $v_z^{\max} = \frac{3}{2}v_{z,\text{average}}$; PF ($N_{Re} \gg 750$): $v_z^* = 1$, $v_z^{\max} = v_{z,\text{average}}$; SF ($N_{Re} < 750$): $v_z^* = 1-(2\xi^*-1)^2$, $v_z^{\max} = \frac{3}{2}v_{z,\text{average}}$ Geometrically thick annular photoreactors ($0 < \eta < 1$)—SF ($N_{Re} < 2000$): $v_z^* = \frac{1-(r^*)^2+2(\eta_{V_{\max}})^2\ln(r^*)}{1-((\eta_{V_{\max}})^2/2)[1-\ln((\eta_{V_{\max}})^2/2)]}$; $r^* = \eta+(1-\eta)\xi^*$; $2(\eta_{V_{\max}})^2 = \frac{1-\eta^2}{\ln(1/\eta)}$ and $v_z^{\max} = \left\{\frac{2-(\eta_{V_{\max}})^2[1-\ln((\eta_{V_{\max}})^2/2)]}{(1-\eta^4)/(1-\eta^2)-2(\eta_{V_{\max}})^2}\right\}v_{z,\text{average}}$		
Dimensionless LVRPA and radiation model parameters	Level 1 TFS photocatalytic reactors with $\omega < 0.3$	Level 2 TFS photocatalytic reactors, any value of ω	Level 3 "geometrically thick" photocatalytic reactors, any value of ω
Apparent optical thickness	Beer–Lambert's absorption model—$(\text{LVRPA})^* = I_{\xi^*=0,z^*}^* \exp(-\tau_{\text{app}}\xi^*)$, $f(\omega,\tau) = 1$	Two-flux absorption–scattering model—$(\text{LVRPA})^* = I_{\xi^*=0,z^*}^* \exp(-\tau_{\text{app}}\xi^*)$, $f(\omega,\tau) = 1+\frac{1}{\omega}\left(1-\frac{1+\psi}{1-\psi}\sqrt{1-\omega^2}\right)$, $\psi = \frac{1-\sqrt{1-\omega^2}}{1+\sqrt{1-\omega^2}}\exp(-2\tau_{app})$	Six-flux absorption–scattering model—$(\text{LVRPA})^* = I_{\xi^*=0,z^*}^* \frac{\eta}{\eta+(1-\eta)\xi^*}\exp(-\tau_{\text{app}}\xi^*)$, $f(\omega,\tau) = \left(1+\frac{1}{\omega_{\text{corr}}}\left(1-\frac{1+\gamma}{1-\gamma}\sqrt{1-\omega_{\text{corr}}^2}\right)\right)\left(1+\frac{4\omega p_s}{1-\omega p_f-\omega p_b-2\omega p_s}\right)$; $a = 1-\omega p_f-\frac{4\omega^2 p_s{}^2}{(1-\omega p_f-\omega p_b-2\omega p_s)}$; $b = \omega p_b+\frac{4\omega^2 p_s^2}{(1-\omega p_f-\omega p_b-2\omega p_s)}$, $\omega_{\text{corr}} = \frac{b}{a}$; $\gamma = \frac{1-\sqrt{1-\omega_{\text{corr}}^2}}{1+\sqrt{1-\omega_{\text{corr}}^2}}\exp(-2\tau_{\text{app}})$
	$\tau_{app} = \tau$	$\tau_{\text{app}} = \tau\sqrt{1-\omega^2}$	$\tau_{\text{app}} = a\tau\sqrt{1-\omega_{\text{corr}}^2}$
Kinetic equation, material balance and Damköhler number	$-r_j = k_{\text{T}}\,(\text{LVRPA})^m(C_j)^n$; $v_z^*\frac{\mathrm{d}C_j^*}{\mathrm{d}z^*} = -N_{Da}(\text{LVRPA}^*)^m(C_j^*)^n$; $N_{Da} = \frac{k_T(\text{LVRPA}_{\xi^*=0}^{\max})^m H(C_j^{\text{in}})^{n-1}}{v_z^{\max}}$		
Radial distribution of substrate concentration at reactor outlet	Thin-film annular photoreactors ($\eta \approx 1$)— $C_{j,\xi^*}^{*\text{out}} = \left[1-A\frac{N_{Da}(1-n)\exp(-m\tau_{\text{app}}\xi^*)}{v_z^*}\right]^{1/1-n}$ for $n \neq 1$; $C_{j,\xi^*}^{*\text{out}} = \exp\left[1-A\frac{N_{Da}\exp(-m\tau_{\text{app}}\xi^*)}{v_z^*}\right]$ for $n = 1$ Geometrically thick annular photoreactors ($0 < \eta < 1$)— $C_{j,\xi^*}^{*\text{out}} = \left[1-A\left(\frac{\eta}{\eta+(1-\eta)\xi^*}\right)^m\frac{N_{Da}(1-n)\exp(-m\tau_{\text{app}}\xi^*)}{v_z^*}\right]^{1/1-n}$ for $n \neq 1$, $C_{j,\xi^*}^{*\text{out}} = \exp\left[1-A\left(\frac{\eta}{\eta+(1-\eta)\xi^*}\right)^m\frac{N_{Da}\exp(-m\tau_{\text{app}}\xi^*)}{v_z^*}\right]$ for $n = 1$		
Geometrical coefficient	$A = \int_0^1 (I_{\xi^*=0,z^*}^*)^m\,\mathrm{d}z^*$; if $m = 1$ we have: $A_{m=1} = \left(\beta(\alpha+1)\arctan\left[\frac{\beta}{2}(\alpha+1)\right]-\beta(\alpha-1)\arctan\left[\frac{\beta}{2}(\alpha-1)\right]+\ln\frac{1+[(\beta/2)(\alpha-1)]^2}{1+[(\beta/2)(\alpha+1)]^2}\right)(2\alpha\beta\arctan\left(\frac{\beta}{2}\right))^{-1}$		

Table 1 (*Continued*)

Conversion	Thin-film annular photoreactors ($\eta \approx 1$)—$\gamma_j = 1 - \frac{v_z^{\max}}{v_z^{\text{average}}} \int_0^1 v_z^* C_{j,\xi^*}^{*\text{out}} \, d\xi^*$
	Geometrically thick annular photoreactors ($0 < \eta < 1$)—
	$\gamma_j = 1 - \frac{2}{(1+\eta)} \frac{v_z^{\max}}{v_z^{\text{average}}} \int_0^1 [\eta + (1-\eta)\xi^*] v_z^* C_{j,\xi^*}^{*out} d\xi^*$
Absorbed radiant power	$W_{\text{abs}} = 2\pi A_{m=1} H \eta R [1 - \exp(-\tau_{\text{app}})] I_{\xi=0}^{\max} (1-\omega) \frac{\tau}{\tau_{\text{app}}}$
Radiation transmission factor	$\Psi = \frac{W_{\text{abs}}}{W_{\text{lamp}}} = \frac{2}{\pi} A_{m=1} \alpha [1 - \exp(-\tau_{\text{app}})] \arctan\left(\frac{\beta}{2}\right) (1-\omega) f(\omega, \tau) \frac{\tau}{\tau_{\text{app}}}$

In thin-film photoreactors the thickness of the reaction space is of the order of one millimeter or less and $\eta \approx 1$. As a result, the effect of lateral scattering of the photons and the effect of curvature on photon fluxes and fluid flow can be safely neglected. In ''geometrically thick'' photoreactors, $0 < \eta < 1$, therefore the effect of lateral scattering of the photons and the effect of curvature on photon fluxes and fluid flow must be taken into account. These two cases will be dealt below using either a two or a six-flux absorption–scattering model.

3.2. Radiation emission model

The emission of radiation from the lamp is modeled using the Linear Source Spherical Emission (LSSE) model [19]. The lamp is considered to be a line source. Each point on this line is assumed to emit radiation in every direction and isotropically. There is no light absorption, scattering, or emission in the space between the lamp and the inner radius of the annulus. The LSSE model is preferred to more complex radiation emission models as it allows a reasonable representation of the radiation field at the inner wall of the annulus and allows a significant simplification of the mathematical model.

According to the LSSE model the intensity of the incident radiation entering the inner wall of the annulus can be written as follows:

$$I_{(\eta R),z^*} = \frac{S_l}{4\pi\eta R} \left\{ \arctan\left[\frac{\beta}{2}(2\alpha z^* - \alpha + 1)\right] - \arctan\left[\frac{\beta}{2}(2\alpha z^* - \alpha - 1)\right] \right\}, \tag{6}$$

where S_l is the radiation emission of the lamp per unit time and unit length of the lamp:

$$S_l = 2\pi r_l \int_{\lambda_{\min}}^{\lambda_{\max}} I_{w,\lambda} \, d\lambda \tag{7}$$

Eq. (6) shows that the photonic flux at the inner wall of the annulus is not uniform along the z direction. It is worth noting that Eq. (7) considers only the photons emitted by the lamp, and therefore does not include radiation from the scattering effects that take place within the reaction space.

According to the LSSE model the dimensionless intensity of the incident radiation at the inner wall of the annulus can be represented by the equation shown in Table 1.

3.3. Radiation absorption–scattering model

In Table 1, the dimensionless intensity of the incident radiation ($I^*_{\xi^*,z^*}$) is defined as the ratio of the total photon flux at a point (ξ^*, z^*) in the reaction space divided by the maximum value of the photon flux in the reaction space, which in a symmetrical photoreactor system corresponds to the value of the total incident flux calculated at the front window of the photoreactor ($\xi^* = 0$) at the middle length ($z^* = 0.5$). Since the LVRPA is defined as the product of the total photon flux multiplied by the volumetric absorption coefficient, it turns out

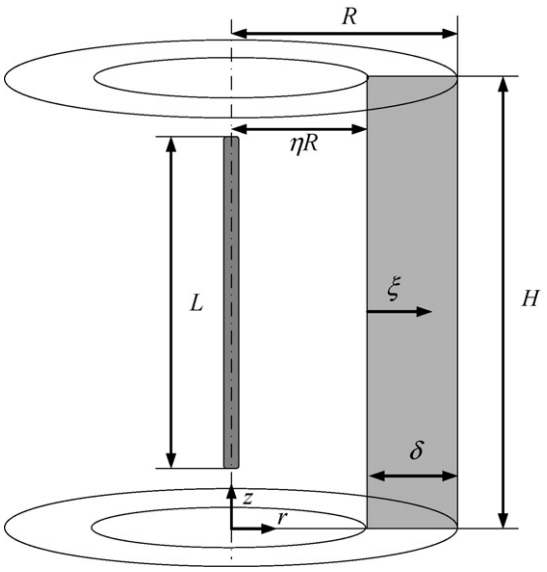

Fig. 1. Schematic representation of the geometry of an annular photocatalytic reactor.

that the dimensionless intensity of incident radiation corresponds to the dimensionless LVRPA.

The two most important dimensionless parameters for the modeling of a photocatalytic reactor are the scattering albedo, ω, which relates to the optical properties of the photocatalyst, and the optical thickness of the reaction space, τ, which is a measure of the degree of opacity of the photoreactor.

The scattering albedo is defined as the ratio of the scattering coefficient, divided by the extinction coefficient of the photocatalyst suspension (Table 1), where α and κ are the specific mass scattering and absorption coefficients, respectively. As these are wavelength-dependent quantities, the analysis that follows is meant to be for monochromatic irradiation. In the case of polychromatic radiation the two quantities may be averaged over the useful spectrum of the incident radiation:

$$\sigma = \frac{\int_{\lambda_{min}}^{\lambda_{max}} \sigma_\lambda I_\lambda \, d\lambda}{\int_{\lambda_{min}}^{\lambda_{max}} I_\lambda \, d\lambda} \quad (8)$$

$$\kappa = \frac{\int_{\lambda_{min}}^{\lambda_{max}} \kappa_\lambda I_\lambda \, d\lambda}{\int_{\lambda_{min}}^{\lambda_{max}} I_\lambda \, d\lambda}, \quad (9)$$

where λ_{min} and λ_{max} are respectively the minimum and maximum wavelengths of the incident radiation that can be absorbed by the photocatalyst. However, caution should be exerted in this case, especially when using lamps with irregular emission spectra, as using the averaged quantities is clearly not rigorous and may lead to errors. Also, note that the scattering albedo should be evaluated using the absorption and scattering coefficients determined experimentally under the prevailing conditions of the slurry suspension (i.e., with the observed degree of agglomeration of TiO_2 in the suspension).

The optical thickness of the photoreactor (Table 1) is a function of the extinction coefficient ($\sigma + \kappa$), the thickness of the reaction space δ or $[R(1 - \eta)]$ and the concentration of photocatalyst c_{cat}. The optical thickness takes the physical meaning of the ratio of the thickness of the reaction space divided by the photons mean free path in the suspension. The experimental methods for the measurement of the extinction coefficient ($\sigma + \kappa$) and of the scattering albedo ω have been reported in the literature [20,21].

Model simulations have shown that when $\omega < 0.3$ or smaller, in practice the effect of radiation scattering can be safely neglected in the modeling procedure [11,22]. Under the above circumstances, the dimensionless LVRPA in the reaction space takes the form shown in Table 1, which is similar to the ''Beer–Lambert'' law. As a result, a simple dimensionless analysis of the reactor can be performed. It is worth noting that the attenuation term of (LVRPA)* in the radial direction is expressed in terms of the optical thickness of the reaction space ($\tau_{app} = \tau$).

Although the case for $\omega < 0.3$ results in readily applicable analytical equations, its applicability in the modeling of photocatalytic reactors is rather limited since commercial photocatalysts (i.e., TiO_2 powders) typically have scattering albedo higher than 0.5 [20,21]. This implies that the radiation scattering phenomena should be included in the modeling of photocatalytic reactors. Nevertheless, the above model can be useful for an ''optimistic'' analysis of the performance of photocatalytic reactors. Since radiation scattering always reduces the number of photons absorbed within the reaction space of a photocatalytic reactor, it can be expected that the performance of a photocatalytic reactor in the presence of scattering will be poorer compared to the case in which radiation scattering has been neglected (see also Figs. 5 and 6).

As mentioned above, the applicability of a simplified radiation–scattering model would depend on the geometry of the reactor. A suitable radiation absorption–scattering model for TFS photocatalytic reactors is the two-flux model (TFM) [11]. This is a one-dimensional radiation model in which the incident radiation at a point (ξ^*, z^*) in the liquid film is taken to be equal to the sum of the radiation flux that travels in the forward direction and the fraction that travels in the backward direction due to back-scattering (Fig. 2). The traveling direction of these photon fluxes is taken to be orthogonal to the main liquid flow direction.

The dimensionless LVRPA at a point (ξ^*, z^*) in the reaction space calculated with the TFM takes the same form as for the case without back-scattering (Table 1) but with the introduction of a dimensionless function $f(\omega, \tau)$ and of an ''apparent'' optical thickness. This function depends on the scattering albedo ω and on the optical thickness τ. The expression for $f(\omega, \tau)$ for the case

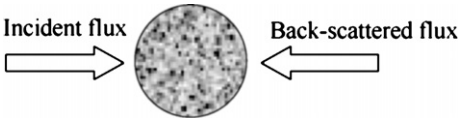

Fig. 2. Photon fluxes in the TFM.

of pure back-scattering can be derived from the study of Brucato and Rizzuti [11] under the assumption that the optical thickness of the photoreactor is large enough to make ψ a small number such that $(1-\psi)\approx 1$ This is the case of an optically thick photoreactor, which corresponds to negligible radiation flux leaving from the outer wall of the annulus as it would be expected in commercial photoreactors. The TFM shows that the attenuation term of the (LVRPA)* is a function of the ''apparent optical thickness'' of the reaction space. This is related to the ''characteristic extinction length'' of photons when radiation scattering is present and corresponds to the optical thickness, which would be measured using a thin-film photoreactor system with scattering particles.

''Geometrically thick'' photoreactors are those reactors in which the thickness of the reaction space cannot be neglected in comparison with the other dimensions of the reactor. An example is the annular photoreactor used in many research laboratories for kinetic studies. To model these types of reactors we have recently introduced a novel six-flux absorption–scattering model (SFM) [14,15], which is a three-dimensional extension of the two-flux model, used to model TFS photoreactors. The SFM allows an integral analytical estimation of the local volumetric rate of photon absorption (LVRPA) at each point of the reactor. The SFM has shown close agreement with the Monte Carlo simulation of the radiation field in a planar photoreactor [15]. This model takes into account both absorption and scattering of photons. The main assumption of this model is that photons are either absorbed or scattered upon colliding with a particle, and scattering follows the route of one of the six directions of the Cartesian coordinates (Fig. 3).

The derivation of the SFM from first principles and its experimental validation is reported in Li Puma et al. [14] and Brucato et al. [15]. The LVRPA calculated with the SFM using the nomenclature reported in their paper is:

$$e^{a}_{r,z} = \frac{I_O}{\lambda_{\omega corr}\omega_{corr}(1-\gamma)} \times \frac{\eta}{r^*}\left[(\omega_{corr}-1+\sqrt{1-\omega^2_{corr}})e^{-R(r^*-\eta)/\lambda_{\omega corr}} + \gamma(\omega_{corr}-1-\sqrt{1-\omega^2_{corr}})e^{+R(r^*-\eta)/\lambda_{\omega corr}}\right] \quad (10)$$

In Table 1 the SFM is reported in dimensionless form for an optically thick photoreactor, i.e., negligible radiation flux leaving from the outer wall of the annulus and $(1-\gamma)\approx 1$. The model parameters p_b, p_f and p_s of the SFM are the probability of backward, forward and side scattering. These can be estimated by fitting the SFM to the exact solution of the radiative transfer equation by a Monte Carlo approach. For the case of a ''diffusively reflecting large sphere'' phase function [23] given by:

$$\Phi(\varphi) = \frac{8}{3\pi}(\sin\varphi - \varphi\cos\varphi), \quad (11)$$

p_b, p_f and p_s were found to be equal to 0.71, 0.11 and 0.045, respectively [15].

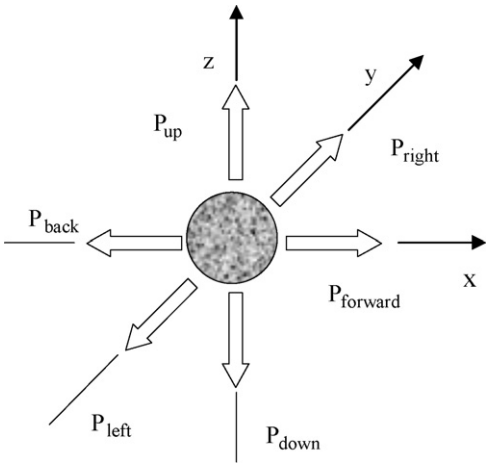

Fig. 3. The six principal directions of photons scattering in the SFM and the scattering probabilities.

The use of the diffusively reflecting large sphere phase function (Eq. (11)) in TiO_2 slurry photoreactors has been recently questioned [21,24] and other phase functions, including the simple isotropic scattering phase function (i.e., p_b, p_f and $p_s = 1/6$ for SFM) have been claimed to better approximate the real optical behaviour of TiO_2 slurries. The matter however is not settled yet. As the scattering phase function strongly depends on particle size distribution and particle morphology, and the latter depend in turn on a number of variables such as TiO_2 type, particle concentration, aggregate agglomeration/breakage dynamics, liquid phase composition, pH, turbulence intensity, etc., no general phase function can be proposed. An interesting possibility is that of using a fairly general function with an adjustable parameter, as proposed by Satuf et al. [21]. However, for the purpose of the present work, Eq. (11) was adopted. In reality, the procedure is independent of the choice of a particular phase function, and may easily be adapted to any phase function by simply adjusting the values of the three parameters p_b, p_f and p_s. This may expected to lead to different quantitative results (e.g., the exact value of the optimal catalyst loading), but the qualitative conclusion of this work (e.g., the existance of such an optimum, and its dependence on reactor features) should not be affected by the phase function.

The SFM, as shown in Table 1, was derived under the assumption that the intensity of the incident radiation at the inner wall was approximately constant for an axial length of the reactor equal to the thickness of the annulus, and that the average travelling path length of scattered photons in the axial direction was always much less than the thickness of the annulus. These assumptions are rational for an annular photocatalytic reactor of optimal geometry, i.e., the geometrical design parameter α and β have been selected such that the axial change in $I_{(\eta R),z^*}$ is small for the majority of the length of the reactor (e.g., $\alpha = 1.3$ and $\beta = 20$) [22] and that it is operating at optimal optical thicknesses ($\tau_{app} > 1$). The function $f(\omega, \tau)$ with the SFM takes into account that the intensity of the incident radiation at each point of the reaction space arrives from the forward flux, the back and the side scattered fluxes.

As shown with the TFM, the attenuation term of (LVRPA)* with the SFM is a function of the ''apparent optical thickness'' of the reaction space. This is related to the ''characteristic extinction length'' of photons when radiation scattering is present and corresponds to the optical thickness, which would be measured using a geometrically thick photoreactor system with scattering particles.

The TFM and the SFM form the basis for a simplified, yet realistic, mathematical representation of the radiation field in annular photocatalytic reactors in the presence of absorbing–scattering particles.

3.4. Fluid-dynamics models

The liquid phase is considered to be a Newtonian fluid with constant physical properties. The catalyst particles are considered to be uniformly distributed within the liquid film; however, the concentration of solids is not so high as to cause substantial changes in the rheological properties of the fluid. The entrainment of gas bubbles is limited and the effect of the velocity gradients on the radial particle distribution is negligible. The dimensionless velocity is represented by:

$$v_z^* = \frac{v_z}{v_z^{\max}} \tag{12}$$

The flow regime for the fluid is determined by the value of Reynolds number, N_{Re}, as shown in Table 1 [25].

For thin-film photoreactors, three cases of steady-state, unidirectional, continuous flow have been considered in the model as shown in Table 1: falling film laminar flow (FFLF), plug flow (PF) and slit flow (SF). Conversely, in geometrically thick photoreactors the fluid flow is taken to be fully developed slit flow (Table 1). In geometrically thick photocatalytic reactors the thickness of the annulus should be of the order of centimetres or less, since operation at high catalyst concentration is desirable in order to maximize the concentration of hydroxyl radicals per unit volume. If this is coupled with limitation to the maximum allowable flow rate, imposed by the material of construction of the UV transparent inner wall (quartz or pyrex), the regime of slit flow is most often verified.

3.5. Reaction kinetics

The kinetic equation for the photocatalytic degradation of a species j in Table 1 can be derived from the literature [26]. At each point in the reaction space, the rate of the reaction of a substrate j is taken to be proportional to the LVRPA raised to the mth power and to the nth power of the local substrate concentration C_j. The parameter m is linked to the efficiency of electron-hole formation and recombination at the catalysts surface and takes a value between 0.5 and 1. The method for obtaining m and n is based on the approximation that the conversion per pass is small [14]. k_T is a constant that takes into account all other factors that may affect the overall quantum yield, with the exception of the substrate concentration and the LVRPA. A discussion for using a power law kinetic equation in preference to a more popular Langmuirian rate equation has been given elsewhere [14]. It is clearly important to avoid employing oversimplified kinetic models, as this may significantly affect model results. On the other hand, it is only with simplified models that analytical (closed form) solutions may be obtained. As a consequence the adoption of models able to properly account for the dependence on the major factors affecting the process may well be a good choice, as the relevant loss of precision may well be compensated by the advantages of dealing with simpler closed form solutions.

3.6. Material balance

The dimensionless material balance for a substrate j in Table 1 was derived taking a differential, annular control volume within the liquid film, and neglecting the transversal diffusive flux term. This simplification is required in order to obtain closed form model equations, and is based on the consideration that photocatalytic reactions, being kinetically quite slow reactions, often result in negligible radial gradients of C_j. There may well be cases, however, where this assumption is not realistic. These should be treated with models able to account for such effects. The material balance is expressed in terms of the Damköhler number, N_{Da}, which in this case has the meaning of the ratio of the overall reaction rate, calculated at the inlet concentration and at the maximum photon flux, to the maximum input mass flow rate of the reactant.

The integration of the design equation with initial condition:

$$z^* = 0, \qquad C_j^* = 1 \tag{13}$$

yields the radial distribution of the dimensionless concentration of substrate j at the reactor outlet section, $C_j^{H^*}$ from which the conversion can be calculated.

A is a dimensionless coefficient that depends only on m and reactor geometry and an analytical solution is possible when $m = 1$ as shown in Table 1.

3.7. Radiation absorption and radiation transmission factor

The effective radiant power absorbed within the reaction space W_{abs} can be obtained by integrating the LVRPA in the reaction space.

$$\begin{aligned} W_{abs} &= \int_V (\mathrm{LVRPA})\,\mathrm{d}V = 2\pi \int_{\eta R}^{R} \int_0^H r(\mathrm{LVRPA})\mathrm{d}r\,\mathrm{d}z \\ &= 2\pi H(R-\eta R) \\ &\quad \times (\mathrm{LVRPA})_{\xi^*=0}^{\max} \int_0^1 \int_0^1 [\eta R \\ &\quad + (R-\eta R)\xi^*](\mathrm{LVRPA})^* \mathrm{d}\xi^*\,\mathrm{d}z^* \end{aligned} \tag{14}$$

The result of the integration is shown in Table 1. Once the absorption of radiation W_{abs} is known, the apparent quantum yield of a photocatalytic reaction can be calculated.

The radiant power emitted by the radiation source, i.e., the UV lamp, W_{lamp} can be calculated by considering the total

photon flux at the inner wall of the reactor using the LSSE model (Eq. (6)):

$$W_{(\eta R)} = 2\pi(\eta R)\alpha L \int_0^1 I_{(\eta r),z^*}\, \mathrm{d}z^* = A_{m=1} S_l \alpha L \arctan\left(\frac{\beta}{2}\right) \tag{15}$$

and letting $\alpha = 1$, $\beta \to \infty$ in Eq. (15) and replacing (ηR) with r_l. It follows:

$$W_{\text{lamp}} = \frac{\pi}{2} S_l L = \frac{\pi}{2} 2\pi r_l L \int_{\lambda_{\min}}^{\lambda_{\max}} I_{w,\lambda}\, \mathrm{d}\lambda \tag{16}$$

The efficiency of photon utilization in annular photocatalytic reactor can be represented by the radiation transmission factor Ψ, that is, the ratio of W_{abs} divided by W_{lamp} and the result is shown in Table 1.

3.8. Dimensionless groups

The models in Table 1, are expressed in term of four dimensionless groups. These are, the Reynolds number, N_{Re}, which suggests the type of fluid-dynamic model (laminar or turbulent flow) to be included in the model, the Damkohler number, $N_{Da} \ll 1$ indicates that the disappearance of the substrate j is much slower than the convective transport through the reactor, the (apparent) optical thickness of the photoreactor τ (or τ_{app}) which is a measure of the degree of opacity of the photoreactor, and the scattering albedo of the photocatalyst, ω, which relates to the optical properties of the photocatalyst. The above dimensionless groups should be maintained constant, if possible, during scale-up of photocatalytic reactors by dimensional analysis.

The expression of the model in dimensionless form allows the analysis of the effect of these dimensionless groups on reactant conversion.

4. Comparison of TFM and SFM predictions

The model predictions of TFM and SFM are compared as a function of the dimensionless groups and dimensionless parameters. To allow a comprehensive analysis of the effect of each dimensionless group, the geometrical parameters were selected to be $\alpha = 1.3$, $\beta = 20$ in all simulations, which represents a suitable geometry of a pilot-scale annular photoreactor.

4.1. Radiation transmission factor

Fig. 4 shows the values of the radiation transmission factor (efficiency of photon utilization), Ψ, as predicted with the TFM and SFM as a function of the optical thickness, τ (Fig. 4a) and of the apparent optical thickness, τ_{app} (Fig. 4b) at different values of the scattering albedo. As expected, the TFM is found to underestimate the absorbed photon flux in comparison with the SFM, whose predictions should be expected to be quite close to reality, if a plane geometry system were considered. For the cylindrical geometry, under consideration here, it may be suggested that SFM predictions are likely to overestimate somewhat the absorbed flux, since in the plane slab geometry none of the side scattered photons is allowed to escape the system, while in the cylindrical geometry, this is bound to occur to some extent. It may be concluded that the real reactor behaviour probably lies in between the TFM and SFM predictions, being probably closer to the latter.

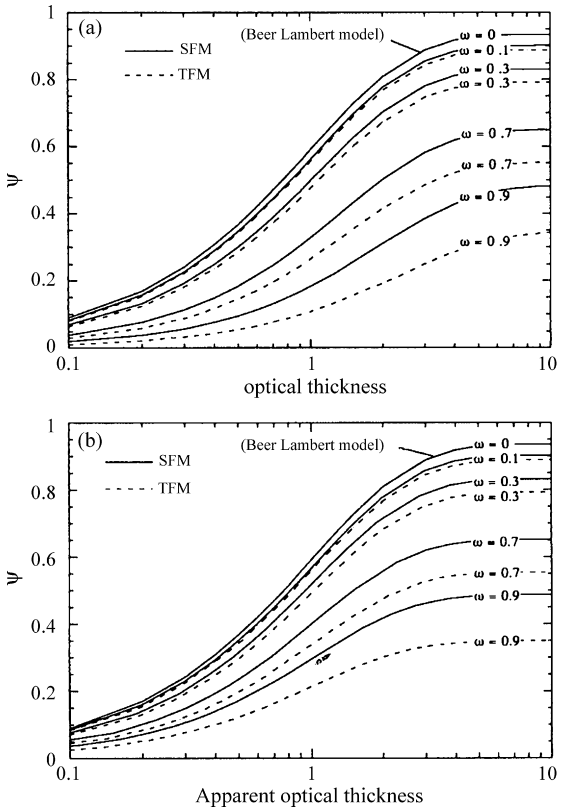

Fig. 4. Radiation transmission factor, Ψ, as predicted with the TFM and SFM as a function of the optical thickness, τ (Fig. 5a) and of the apparent optical thickness, τ_{app} (Fig. 5b) at different values of the scattering albedo. Geometrical parameters: $\alpha = 1.3$, $\beta = 20$.

The radiation transmission factor increases with the (apparent) optical thickness until an asymptotic plateau is reached which occurs at progressively lower values, as the scattering albedo increases. Note that when $\omega = 0$ (no radiation scattering) Ψ does not reach unity since in the geometry under consideration ($\alpha = 1.3$, $\beta = 20$) some photons are allowed to escape from the top and bottom ends of the photoreactor through the space between the lamp and the inner wall of the annulus. Furthermore, Fig. 4a shows that this plateau is reached at increasing values of the optical thickness as the scattering albedo increases and it is a function of the geometry of the reactor (Table 1). Conversely, in Fig. 4b the plateau is reached at the same values of the apparent optical thickness regardless of the value of the scattering albedo. It also shows that there is little benefit in operating the reactor at apparent optical thicknesses higher than approximately 3. However, the precise value of apparent optical thickness at which to operate a photocatalytic reactor depends on the reaction kinetics and type of flow pattern as it will be shown in following sections.

In Fig. 4b it can be seen that the uncertainty in the estimation of Ψ, i.e., the interval between SFM and TFM predictions, remains practically constant for values of $\tau_{app} \geq 2$ and increases with the scattering albedo. When $\omega = 0.5$ the uncertainty is less than 10%, while it becomes approximately 30% when $\omega = 0.8$.

4.2. Idealized flow, reaction kinetics, scattering albedo and conversion

The kinetic parameters m and n in the model correspond to the dependence of the reaction rate of a substrate j on the LVRPA and the substrate concentration, respectively. The langmuirian fitting of the rate data of photocatalytic reactions results in the values $n = 1$ at low substrate concentration (typically <1–10 ppm) and $n = 0$ at high substrate concentration (typically >100 ppm). Kinetic studies on the effect of the intensity of the incident radiation have shown that at weak intensities, typically less than 10^{-3} Ein m^{-2} s^{-1}, the observed rate of oxidation is first order in radiation intensity [27], i.e., $m = 1$. These limiting cases for m and n were used to illustrate the effect of reaction kinetics on the calculated substrate conversions using the TFM and SFM.

If the inlet substrate concentration C_j^{in} is chosen to be 1, the Damköhler number, N_{Da}, is independent of substrate concentration. After rearrangement and replacing of the terms with $m = 1$, it becomes:

$$N_{Da} = \left(\frac{k_T H \arctan(\beta/2) \int_{\lambda_{min}}^{\lambda_{max}} I_{w,\lambda}\, d\lambda}{\eta R^2 (1-\eta) v_{z,average}} \right) \left(\frac{v_{z,average}}{v_z^{max}} f(\omega,\tau)(1-\omega)\tau \right) \quad (17)$$

The first term in parenthesis is independent of scattering albedo, optical thickness and type of flow pattern and was assigned the value 1.2611 in the simulations such that the maximum conversion with the FFLF system in the absence of radiation scattering ($\omega = 0$) was 80%. This choice allows the elucidation of the full effect of the flow conditions and reaction kinetics on conversion.

Figs. 5 and 6 show model simulation results for the conversion of a substrate j calculated with the TFM and SFM as a function of the apparent optical thickness, τ_{app}, at different values of the scattering albedo, and different reaction kinetics, respectively, for FFLF, PF and SF ideal flow systems. Several aspects can be observed from these results.

Figs. 5 and 6 show that radiation scattering significantly affects the conversions obtained at different values of apparent optical thickness. As the scattering albedo ω increases, the conversions decrease significantly as a result of losses of photons from the reacting systems by scattering.

The model simulations show that for given values of the scattering albedo, apparent optical thicknesses and reaction kinetics, the conversions obtained with the three different idealized flow systems follow the sequence: FFLF > PF > SF. The reasons for this have been explained in full elsewhere [21] and can be attributed to the degree of correspondence between radiation field and fluid residence time. For example, in the FFLF system there is a high degree of correspondence between radiation field and fluid residence time since the fluid elements with the lowest residence times near the front wall of the annulus ($\xi^* = 0$) receive maximum intensity of radiation, and the fluid elements with the longer residence times near the back wall ($\xi^* = 1$) receive the lowest intensity of radiation. Conversely, in the SF system there is a low degree of correspondence of radiation field and fluid residence time since the fluid elements with the lowest residence times, near the middle of the wall of the annulus, receive a photon flux that has been attenuated by the previous layers and, therefore, exits the reactor with a low degree of substrate conversion.

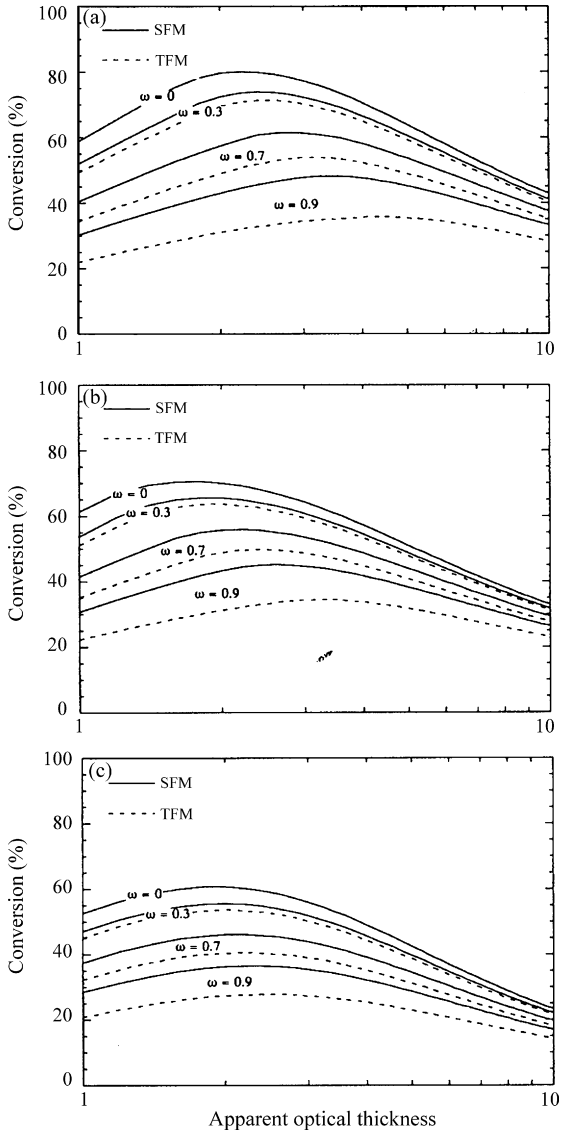

Fig. 5. Model simulations for the conversion of a substrate j calculated with the TFM and SFM as a function of the apparent optical thickness, τ_{app}, at different values of the scattering albedo for different idealized flow conditions. Kinetic parameters: $m = 1$, $n = 1$. Geometrical parameters: $\alpha = 1.3$, $\beta = 20$. (a) FFLF; (b) PF; (c) SF.

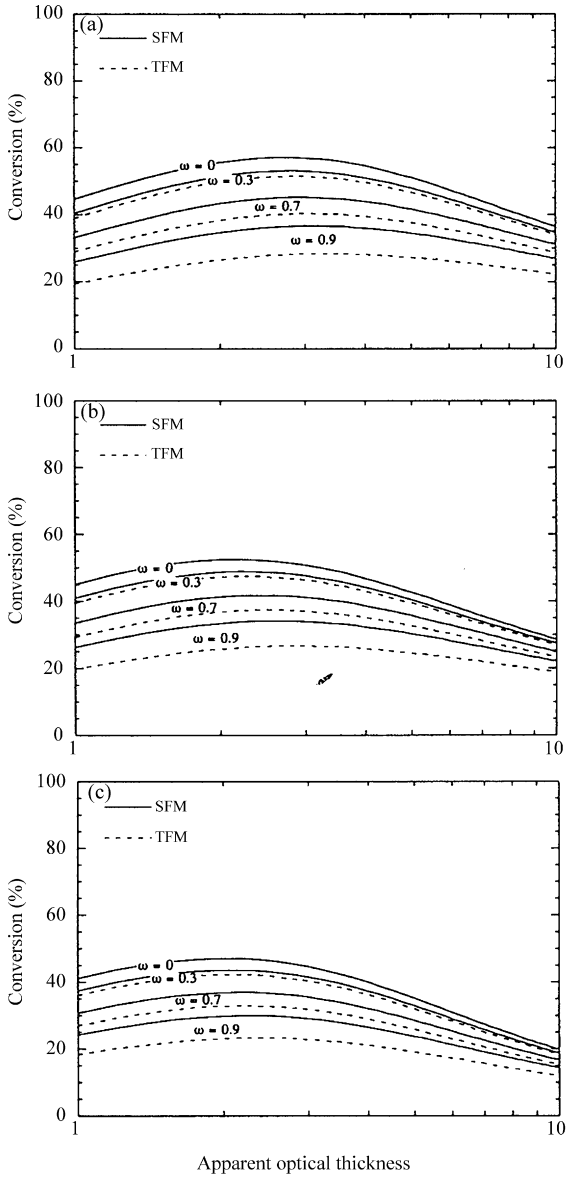

Fig. 6. Model simulations for the conversion of a substrate j calculated with the TFM and SFM as a function of the apparent optical thickness, τ_{app}, at different values of the scattering albedo for different idealized flow conditions. Kinetic parameters: $m = 1$, $n = 0$. Geometrical parameters: $\alpha = 1.3$, $\beta = 20$. (a) FFLF; (b) PF; (c) SF.

The simulation results show that the SFM predicts higher conversion than the TFM because of the higher efficiency of photon utilization as result of the scattering of photons occurring in the lateral direction as well as in the forward and backward directions. As stated previously, the SFM is indeed a more realistic representation of the scattering phenomena in a photocatalytic reactor than the TFM and therefore should predict reaction conversions closer to reality, though with some degree of conversion overestimation due to the cylindrical geometry. It is worth noting, however, that the uncertainty interval between SFM and TFM predictions is practically negligible when the scattering albedo is 0.3 or less, and becomes significant only at very large values of the scattering albedo.

4.2.1. Optimum apparent optical thickness

Of particular interest is the determination of the optimum value of the apparent optical thickness, thus the optimal catalyst loading, at which a particular photocatalytic reactor should be operated [28]. For a given reactor and type of catalyst, the thickness of the annulus and the scattering albedo are fixed parameters. Therefore, the only operating parameter that can be freely varied is the catalyst loading. In order to facilitate selecting the loading of catalyst that maximize conversions, without the need for performing lengthy experiments, model simulations using the TFM and SFM can be carried out. Figs. 5 and 6 show that an optimal value of the apparent optical thickness exists, which maximizes conversion in a photocatalytic reactor. This occurs as a result of the combination of increase in the opacity of the reactor as the catalyst loading is increased and darkening of the back side of the reactor at large catalyst loading. However, unlike batch photoreactors, in flow-through reactors the fluid velocity profile can have a significant influence on the optimal value of the apparent optical thickness. The maximum conversion in Figs. 5 and 6 occurs at progressively larger values of the optical thickness over a relatively narrow range as the scattering albedo is increased. For example, using the SFM in Fig. 5a the optimum optical thickness ranges from 2.2 at $\omega = 0$ to 3.4 at $\omega = 0.9$ with the FFLF velocity profile, in Fig. 5b it ranges from 1.8 at $\omega = 0$ to 2.6 at $\omega = 0.9$ with the PF velocity profile and in Fig. 5c it ranges from 2 at $\omega = 0$ to 2.2 at $\omega = 0.9$ with the SF velocity profile. Since the parameter m is the order of the reaction with respect to the LVRPA, and considering that $m = 1$ is the upper limit, for $0 < m < 1$ there will be an even closer deviation from optimum optical thicknesses as a function of the scattering albedo. From the results presented, it may be concluded that the optimum value of the apparent optical thickness that maximizes conversion in a flow-through photocatalytic reactor should be found in the range from 1.8 to 4.4 depending on flow conditions and reaction kinetics. Notably, both TFM and SFM give rise to similar results as concerns the optimum optical thickness, which can therefore be considered as well assessed, despite the approximations affecting the two models. As the TFM is a singularity of the SFM with $p_b = 1$, $p_f = p_s = 0$, the difference in the results obtained with the two models may be regarded as indicative of the differences that may result from ‘‘large’’

Table 2
Model parameters used in the simulations

Geometry	$\alpha = 1.197$, $\beta = 16.385$, $H = 0.255$ m
Thickness of annulus	$\delta = 6$ mm
Total UVA intensity at lamp wall (8 W Sylvania blacklight blue)	185.2 W m^{-2}
Substrate initial concentration	$C_j^{in} = 7.495 \times 10^{-3}$ kg m^{-3}
Reynolds number	$N_{Re} = 563$ (laminar flow)
Flow rate	1.7 L min^{-1}
TiO_2 extinction coeff. (Degussa P25)	$(\sigma + \kappa) = 1296$ m^2 kg^{-1}
Scattering albedo	0.7396
Kinetic parameters	$m = 1$, $n = 0.815$, $k_T = 7.5 \times 10^{-6}$ kg$^{(1-n)}$ s^{-1} m$^{3m+3n-3}$ W^{-m}
Catalyst concentration	0.4 kg m^{-3}
Optical thickness	3.114

changes of the scattering phase function. It is therefore confirmed that although the quantitative results are affected by the choice of the phase function, the qualitative features of the results presented (e.g., the existence of an optimal optical thickness and its dependence on other model parameters) may be considered as well assessed.

4.3. Fitting the Beer–Lambert's model, the TFM and SFM to experimental results

In Table 1, it can be observed that the SFM reduces to the TFM by setting $p_b = 1$, $p_f = 0$ and $p_s = 0$ (back-scattering only) and that both TFM and SFM reduce to the Beer–Lambert's absorption model when the scattering albedo ω approaches the value of zero. To illustrate the prediction of experimental results and appreciate the relative error among these three radiation models, these models were compared with the experimental results for the oxidation of the herbicide isoproturon, in aqueous suspensions of TiO_2 (Degussa P25), which have been reported in the literature [14]. The reaction was carried out in an annular photocatalytic reactor operated in a recirculation batch mode. Table 2 summarizes the model parameters and the experimental conditions for the oxidation reaction.

The models were applied to the recirculation system following the method reported in Li Puma et al. [14] and the results are reported in Fig. 7 against the experimental results. In the Beer–Lambert model simulation, the scattering albedo was set equal to zero. The kinetic constant k_T in Table 2 corresponds to that calculated by fitting the SFM to the experimental results of the oxidation of isoproturon under a wide range of experimental conditions [14], therefore a good fit of the experimental results was expected. In Fig. 7 it can be observed that the TFM underestimate the degradation of isoproturon and that the Beer–Lambert model overestimates the experimental results, which is as expected. The TFM and the Beer–Lambert model practically enclose the experimental results. It is however, important to appreciate the relative error among the three radiation models which can be significant and should not be ignored at least for the Degussa P25 photocatalyst.

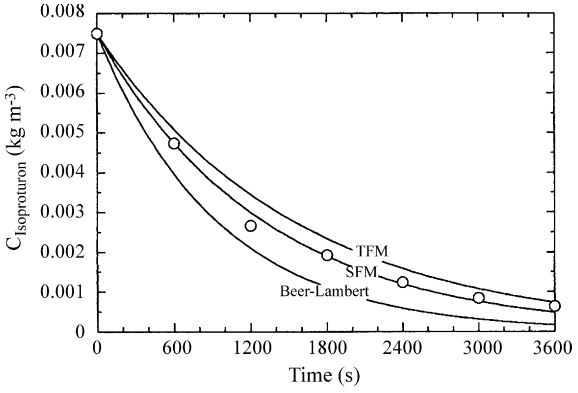

Fig. 7. Modeling the photocatalytic oxidation of isoproturon using Beer–Lambert model, TFM and SFM. Lines are model results with parameters from Table 2. Experimental results are from ref. [14].

The derivation of reaction kinetic constants of photocatalytic reactions should always take into account, as a prerequisite, the mathematical modeling of the radiation field in the reactor. It is evident from this example that the most accurate radiation model is necessary to derive precise values of the kinetic constants. For design purposes, the TFM provides an underestimation of the degradation and therefore can be used as a modeling tool for safe design of photocatalytic reactors. Conversely, ignoring radiation scattering in a photocatalytic reactor can result in significant undersizing of photocatalytic reactors or miss determinations of reaction kinetics constants from experimental reactors.

5. Conclusions

In this work, a dimensionless analysis of steady-state, continuous flow, photocatalytic reactors was performed, by suitably coupling mass and momentum balance results with simplified reaction kinetics and radiation absorption–scattering models. These latter ranged from a simple Beer–Lambert model (no photon scattering), to "two-flux" (scattered photons are purely back scattered) and "six-flux" (scattered photons follow the route of the six directions of the Cartesian coordinates) models. Although at the expense of some approximations, these simplified models retain the essential elements of a rigorous approach, whilst providing simple solutions.

The effect of scattering albedo, ω, and "apparent" optical thickness, τ_{app}, over reactant conversion in a flow-through photocatalytic reactor was analysed using the above models for three ideal flow conditions: (1) falling film laminar flow, (2) plug flow and (3) slit flow.

Simulation results show that for each given flow and geometrical condition, optimum values of τ_{app} (i.e., optimum loading of catalyst particles) exist, at which reactant conversion is maximised. The actual value is a complex function of fluid flow and reaction kinetics, but is usually found in the range from 1.8 to 4.4. Notably the optimal values predicted by the TFM and SFM radiation models are not significantly different. As the two models are expected to enclose the real behaviour of the system, with the SFM being closer to reality than the TFM, the above consideration implies that the optimal optical thickness values can be accepted with confidence. From a qualitative and quantitative point of view, it may also be speculated that the selection of a different scattering phase function, such as the isotropic or the preferential forward scattering as suggested by some authors [21,24] should yield optimal values of τ_{app} which are slightly smaller than the one calculated using the diffusively reflecting large sphere phase function adopted in this work, thus the general conclusions reported above should remain valid.

Finally, model results were compared to experimental data for the photocatalytic oxidation of the herbicide isoproturon in a recirculation batch reactor. As expected the experimental results were found to be enclosed by the Beer–Lambert absorption model and the two-flux radiation model, with the six-flux model providing the most accurate, yet simple, analysis of the photocatalytic reactor performance.

This study has demonstrated the importance of performing accurate modeling of the radiation field in slurry photocatalytic reactors, which should be invaluable when analyzing reaction kinetics, for assessing photocatalyst activities and for selecting the optimal catalyst concentration for given reactor geometry and kinetics. In the view of the authors, accurate kinetics studies in photocatalytic slurries cannot be decoupled from the mathematical analysis of the reactor, and a simple tool to perform this analysis has been provided in this work. As a result, reaction kinetic parameters can be estimated with a higher degree of confidence making the corresponding reaction kinetic equations generally applicable to photoreactors of any geometry and size.

The SFM model, as presented, can also be used for design and scale-up of photocatalytic reactors and for the prediction of reactant conversion expected in flow-through photocatalytic reactors.

It may be worth underlining that, apart from the simplifications involved in the radiant field and kinetic models, mass transfer limitations as a result of radial substrate concentration gradients were also neglected. This has no effect on the predicted performance if the reaction is zero order with respect to reagent concentration (i.e., $n = 0$, Fig. 6 results), but might lead to discrepancies in the case of relatively fast photocatalytic reactions. Possible future model improvements include (i) the adoption of different scattering phase functions leading to different values of the SFM scattering probabilities; (ii) the adoption of more accurate kinetic expressions and (iii) the allowance for mass transfer limitations.

Acknowledgement

The authors are grateful to NATO (Grant SfP-977986) for financial support.

References

[1] M.R. Hoffmann, S.T. Martin, W. Choi, D.W. Bahnemann, Chem. Rev. 95 (1995) 69.
[2] Y. Ohko, K.I. Iuchi, C. Niwa, T. Tatsuma, T. Nakashima, T. Iguchi, Y. Kubota, A. Fujishima, Environ. Sci. Technol. 36 (2002) 4175.
[3] J.-M. Herrmann, Catal. Today 53 (1999) 115.
[4] J.-M. Herrmann, Topics Catal. 34 (2005) 49.
[5] O.M. Alfano, D. Bahnemann, A.E. Cassano, R. Dillert, R. Goslich, Catal. Today 58 (2000) 199.
[6] R.J. Brandi, G. Rintoul, O.M. Alfano, A.E. Cassano, Catal. Today 76 (2002) 161.
[7] G. Li Puma, P.L. Yue, Environ. Sci. Technol. 33 (1999) 3210.
[8] A.E. Cassano, C.A. Martin, R.J. Brandi, O.M. Alfano, Ind. Eng. Chem. Res. 34 (1995) 2155.
[9] A.E. Cassano, O.M. Alfano, Catal. Today 58 (2000) 167.
[10] S. Spadoni, C. Stramigioli, F. Santarelli, Chem. Eng. Sci 35 (1980) 925.
[11] A. Brucato, L. Rizzuti, Ind. Eng. Chem. Res. 36 (1997) 4748.
[12] G.B. Raupp, J.A. Nico, S. Annangi, R. Changrani, R. Annapragada, AIChE J. 43 (1997) 792.
[13] G. Li Puma, Environ. Sci. Technol. 37 (2003) 5783.
[14] G. Li Puma, J.N. Khor, A. Brucato, Environ. Sci. Technol. 38 (2004) 3737.
[15] A. Brucato, A.E. Cassano, F. Grisafi, G. Montante, L. Rizzati, G. Vella, AIChE. J. 52 (2006) 3882.
[16] G. Li Puma, Trans. IChemE. Part A 83 (2005) 820.
[17] M. Pasquali, F. Santarelli, J.F. Porter, P.L. Yue, AIChE J. 42 (1996) 532.
[18] A. Brucato, L. Rizzuti, Ind. Eng. Chem. Res. 36 (1997) 4740.
[19] S.M. Jacob, J.S. Dranoff, Chem. Eng. Prog. Symp. Ser. 62 (1966) 47.
[20] M.I. Cabrera, O.M. Alfano, A.E. Cassano, J. Phys. Chem. 100 (1996) 20043.
[21] M.L. Satuf, R.J. Brandi, A.E. Cassano, O.M. Alfano, Ind. Eng. Chem. Res. 44 (2005) 6643.
[22] G. Li Puma, P.L. Yue, Chem. Eng. Sci. 58 (2003) 2269.
[23] R. Siegel, J.R. Howell, Thermal Radiation Heat Transfer, McGraw-Hill, London, 1972.
[24] R.J. Brandi, O.M. Alfano, A.E. Cassano, Chem. Eng. Sci. 54 (1999) 2817.
[25] R.B. Bird, W.E. Stewart, E.N. Lightfoot, Transport Phenomena, second ed., John Wiley & Sons, New York, 2002.
[26] C.S. Turchi, D.F. Ollis, J. Catal. 122 (1990) 178.
[27] D.F. Ollis, E. In, M. Pelizzetti, Schiavello (Eds.), Photochemical Conversion and Storage of Solar Energy, Kluver Academic Publishers, Dordrecht, 1991, pp. 593–622.
[28] C.A. Martin, G. Camera-Roda, F. Santarelli, Catal. Today 48 (1999) 307.